JOURNAL OF Materials CHEMISTRY

Internal photonic crystal lattice structures of planarized opal-patterned chips probed by laser scanning confocal fluorescence microscopy

Vladimir Kitaev, Sébastien Fournier-Bidoz, San Ming Yang and Geoffrey A. Ozin*

Materials Chemistry Research Group, Chemistry Department, University of Toronto, 80 St. George St., Toronto, Ontario, Canada M5S 3H6. E-mail: gozin@alchemy.chem.utoronto.ca

Received 26th November 2001, Accepted 4th February 2002
First published as an Advance Article on the web 4th March 2002

Laser scanning confocal microscopy, advantageous as a non-destructive spatial imaging technique, has been used to probe the internal photonic crystal lattice structure of micron scale core–fluorescein-labeled shell–corona silica microspheres that had been crystallized within anisotropically etched relief patterns in the 100 surface of silicon wafers. Using this method it was possible to determine the three-dimensional positioning of individual microspheres that had been allowed to self-assemble within the confines of square and rectangular shaped pyramidal microwells with sub-micron lateral and vertical spatial resolution. This methodology confirmed that microspheres underwent vectorial crystal growth in the form of a face centered cubic lattice inside the pyramidal microwells in which the 100 face of the photonic crystal was oriented parallel to the 100 surface of the silicon wafer. Furthermore it was feasible to visualize both external and internal defects buried within photonic crystal lattices in the planarized opal-patterned chips.

The physical dimensions of contemporary optical circuits may profoundly shrink in size if planarized optically integrated silicon microphotonic crystal chips are reduced to practice. Such a development is envisioned to disrupt contemporary photonic technologies and revolutionize optical circuit miniaturization analogous to the displacement of traditional electrical circuits by integrated silicon microelectronic chips.[1,2] A goal of our recent photonics materials chemistry research program has been to integrate three-dimensional oriented microphotonic single crystals, having omnidirectional photonic bandgaps in the near infrared telecommunication wavelength region based on silicon and germanium inverse opals[3–5] and opal-patterned silicon chips,[6,7] into functional optical circuits.[8]

Recently we described a directed self-assembly chemistry approach to the planarized opal-patterned chip.[6–8] The method is founded upon geometrically confined colloidal crystallization of microspheres within surface relief patterns in substrates like silicon wafers. In brief, the procedure involves the combined use of microcontact printing and anisotropic wet etching to make surface relief patterns of pre-determined geometry in an oriented single crystal silicon wafer.[6,7] The idea is to control the nucleation and growth of opal-based micron scale single crystal photonic crystals with specified orientation, defined area and thickness, pre-determined structure, and registry housed entirely within the surface relief designs of a single crystal silicon substrate. Approaches used for localizing microspheres, assembling and ordering them exclusively within geometrically well-defined relief designs of microchannels and microwells in the surface of the silicon wafer, and not anywhere else on the wafer surface, include microfluidic and spin-coating directed self-assembly. An attractive feature of these approaches for making planarized microphotonic crystal chips is that they are quick, reproducible, inexpensive and can be easily integrated into existing chip microfabrication facilities.[8] A number of challenges however remain before the utilization of planarized opal-patterned chips becomes a practical proposition for photonic chip manufacture. A major one involves the development of a non-destructive probe capable of visualizing a 3D photonic lattice structure and, therefore, of detecting defects in embedded microphotonic crystals in chips because of the effect they have on optical properties.

Laser scanning confocal microscopy (LSCM) has previously been used to follow crystallization of colloidal suspensions[9,10] as well as to study the effects of template-directed crystallization—colloidal epitaxy—on the orientation of colloidal crystals.[11–13] However, to our knowledge, a study of defects imaged by LSCM inside colloidal crystals has never been reported. Herein we describe for the first time the use of LSCM to visualize a complete microsphere-by-microsphere 3D structure of an opal-patterned silicon chip in which the surface relief designs of microphotonic crystals are composed of core–fluorescein-labeled shell–corona silica microspheres. The fluorescent dye of choice was fluorescein isothiocyanate (FITC) because of its compatibility with the base catalyzed Stöber–Fink–Bohn seeded growth process for making large diameter (>500 nm) core–corona silica microspheres,[4] and its ease of incorporation into silica particles through a coupling reaction with 3-aminopropyltrimethoxysilane.[14] A continuous silica growth technique with reagents added dropwise[15] was used to introduce the dye uniformly into the desired location in the microspheres. The core–shell–corona architecture with dye molecules selectively incorporated at the interfacial region between the internal core and external corona (see Fig. 1c) was chosen to exclude the possibility of FITC leaching out and to allow the introduction of FITC with high yield in the seeded regrowth process. The dye is therefore concentrated in a shell with controlled thickness between the silica core and corona regions rather than being distributed uniformly throughout the silica microsphere, thereby maximizing the spatial resolution of the fluorescent microspheres of the opal structures. Two microsphere batches A and B were synthesized and characterized as described in the Experimental section.

A spin-coating colloidal crystal assembly method,[8] was utilized to grow opal-based microphotonic crystals from these fluorescent core–shell–corona microspheres in both square and rectangular-shaped pyramidal microwells that had been anisotropically etched in the surface of 100 silicon wafers. The etching process created geometrically well-defined microwells that preferentially expose 111 silicon faces and have a

 DOI: 10.1039/b110826n

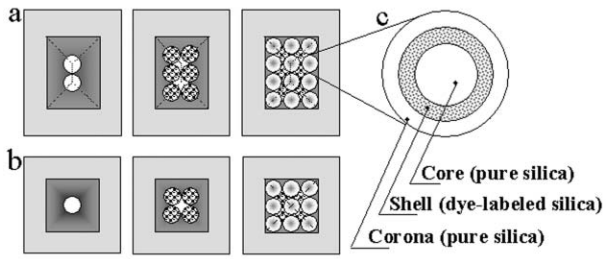

Fig. 1 Schematics of microsphere assembly in geometrically confined (a) rectangular-shaped pyramidal and (b) square-shaped pyramidal microwells in a surface relief patterned 100 silicon wafer with a 70.6° pyramidal angle between the 111 faces of the microwells. Each horizontal series of illustrations shows layer-by-layer filling of the microwell with the microspheres starting from the bottom and progressing to the top. (c) Schematic representation of the architecture of core–fluorescent dye-labeled shell–corona particles used in this work.

pyramidal angle between the faces of the microwell of 70.6°. This confinement geometry forces the imbibed microspheres to adopt the unnatural opal growth direction of 100 parallel to the surface of the silicon wafer.[8] An example of this kind of vectorial control of geometrically directed opal growth is shown schematically in Fig. 1a for a patterned silicon wafer with a 4 × 3 arrangement of microspheres in the top surface. One can observe a perfectly packed single crystal implying three layers of 12, 6 and 2 microspheres from top to bottom. Analogous packing in a square pyramidal well with a 3 × 3 arrangement of microspheres in the top surface with the corresponding three layers of 9, 4 and 1 microspheres from top to bottom is illustrated in Fig. 1b.

LSCM is a method capable of exploring the internal and surface lattice arrangement of microspheres within planarized microphotonic crystals in silicon wafers in a layer-by-layer fashion with vertical and lateral spatial resolution comparable to the microsphere diameter.[16,17] An example that illustrates the *in situ* capability of the method is shown in Fig. 2. When the focal plane of the confocal microscope is located in the surface plane of the silicon wafer the top 3 × 3 rectangular array of nine 900 nm silica microspheres (batch A) is clearly resolved, as seen by inspection of Fig. 2a—interesting and noteworthy one can even discern slight irregularities in the microsphere packing arrangement. We should point out that the observed bright surface of the silicon wafer is not an artifact but instead originates from the luminescence of etched silicon.[5] This luminescence was always present but never interfered with our measurements because the imaged sections of the sidewalls were negligible and only the top surface of the silicon substrate showed bright luminescence due to its large area.

Fig. 2b presents a typical image recorded at intermediate positions between the layers of microspheres in which there is a certain degree of overlapping of layer planes. One has to keep in mind that overlapping of adjacent microsphere layer planes will always be present to a certain extent because of the nature of close packed structures made of layers of interpenetrating microspheres. Closing the pinhole of the confocal optical microscope is helpful but requires using high laser intensity resulting in faster FITC photobleaching. We opted for a compromise, where we can clearly resolve the structure of individual layers and not suffer from excessive photobleaching. In the images shown in Fig. 2, one can readily locate the focal image plane at vertical positions that optimize the resolution of an individual layer of microspheres within the microphotonic crystal contained within the silicon wafer. Inspection of Fig. 2b and c allows clear identification of the second 2 × 2 fluorescent microsphere layer-plane within the square-shaped pyramidal microphotonic crystal. On probing more deeply into the confined opal one observes the bottom point in the pyramid to be the anticipated single fluorescent microsphere shown in Fig. 2d. Thus, probing the surface and bulk microsphere packing arrangement contained within square pyramidal microwells (Fig. 2a–d), reveals a picture consistent with the expected single crystal opal lattice structure (Fig. 1b). Fig. 2e and f provide an example of an "external" defect in the packing of 1 μm silica microspheres (batch B) in square-shaped pyramidal wells, formed during spin-coating using lower than optimal microsphere concentrations. The top plane of the microsphere packing imaged in Fig. 2e has a microsphere missing in the center of the upper row. Inspection deeper inside the microwell, Fig. 2f and g, reveals that the central and bottom layers do not have any vacancies or disorder and that the ideal packing arrangement of microspheres is preserved inside.

One of the main advantages of LSCM is in elucidating "hidden" internal defects not probed by other methods such as the commonly used scanning electron microscopy. Two examples of 1 μm silica microsphere packing with internal defects resolved by LSCM are presented in Fig. 3. The images in Fig. 3a–c show three cross-sections of microspheres arranged in a rectangular 3 μm × 4 μm pyramidal microwell. The top

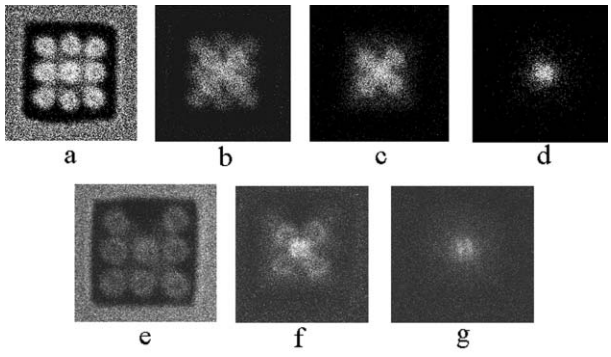

Fig. 2 Laser scanning confocal microscopy images of fluorescein-labeled core–shell–corona silica microspheres packed in square-shaped pyramidal microwells with the top dimension of the microwell in the silicon wafer measuring 3 μm by 3 μm. Each of two series (a) to (d) and (e) to (g) were obtained using 900 nm diameter microspheres (batch A, see text) and 1 μm microspheres (batch B), respectively, and represent optical cross-sections descending from the top to the bottom of the microwells.

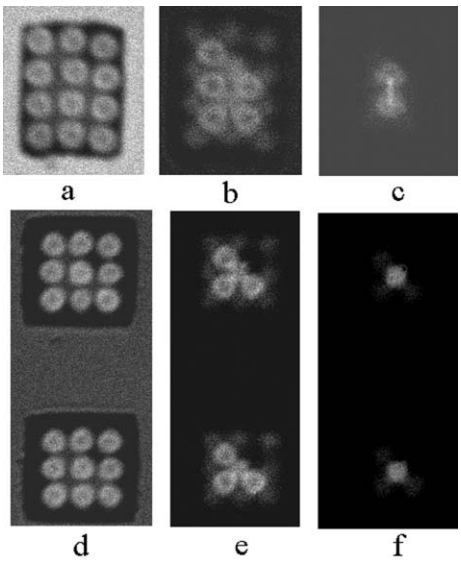

Fig. 3 Laser scanning confocal microscopy images of 1 μm fluorescein-labeled core–shell–corona silica microspheres (batch B, see text) packed in (a) 3 μm by 4 μm rectangular-shaped pyramidal microwell and (d) two 3 μm by 3 μm square-shaped pyramidal microwells, which reveal the presence of "hidden" intrinsic defects in microsphere arrangements. Each of the two series (a) to (c) and (d) to (f) are optical cross-sections descending from the top to the bottom of the microwells.

layer in Fig. 3a is a well-ordered 3 × 4 microspheres array, while the central layer, shown in Fig. 3b with some interference from the top layer, has one sphere missing in the top right corner. Two spheres in the bottom layer (Fig. 3c) are intact and the overall microsphere arrangement is consistent with the expected 100 face centered cubic packing illustrated in Fig. 1a. It can be clearly seen in Fig. 3a, as well as in other images, that the fluorescent dye is distributed as intended during microsphere preparation and is concentrated in the spherical shell region located from roughly half to three quarters of the radius of the microsphere, while the central core and the outer corona are maintained dye-free. Thus, although the outer bright regions are observed not to overlap, the microspheres are actually in physical contact with each other. The core of the microspheres looks darker since the amount of the fluorescent dye in the cross-section through the core is significantly less compared to the fluorescent shell.

Internal defects hidden within microspheres that are packed inside two neighboring square pyramidal wells are shown in Fig. 3d–f. Both the top layer in Fig. 3d and the bottom layer in Fig. 3f are well ordered, however the central layers of both microwells have a missing microsphere located in the same place—see top right corner. A relatively low probability of having the same kind of defect at the same place in the two neighboring microwells suggests the presence of a common type of irregularity in the microwells produced by soft lithography, since as seen in Fig. 3a and d the top right corners of the microwells appear to be similarly distorted.

Finally, two interesting examples of microsphere arrangements in the rectangular-shaped pyramidal microwells filled by spin-coating using low microsphere concentrations are shown in Fig. 4. The upper row of images seen in Fig. 4a–c displays microsphere packing in which the top layer consists of 12 microspheres (Fig. 4a) while the central layer (Fig. 4b) has only 4 microspheres arranged in the corners of the plane and the bottom layer (Fig. 4c) has two microspheres as expected. The observed structure does not correspond to the face centered cubic packing arrangement illustrated in Fig. 1a and likely arises from the kinetics of nucleation and crystallization of microspheres within the geometric confinement of the rectangular-shaped pyramidal microwells. It seems that crystallization was initiated in the top and bottom parts of the microwell simultaneously, thus preventing sites in the center of the middle layer being filled due to geometric constraints of the microspheres already present. Arrangements of microspheres contained in partially filled rectangular-shaped pyramidal microwells shown in Fig. 4d–f support this point of view. Using spin-coating conditions with low microsphere concentrations results in microspheres preferentially occupying the edges of the microwell, which are the most favorable places for spheres to be anchored since they can interact with two faces of the microwell simultaneously. In a similar fashion, we observed that the first sphere to fill a square pyramidal microwell always prefers to be located at the bottom. Preferential filling of the bottom and edges demonstrates the importance of the geometric parameters of confinement for the microsphere packing as well as the conditions of microwell filling, that are, microsphere concentrations and spin-coating conditions.

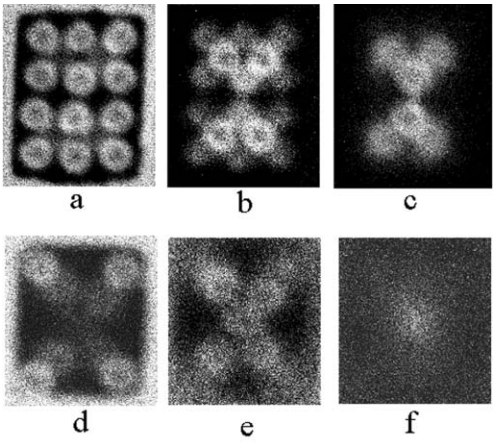

Fig. 4 Laser scanning confocal microscopy images demonstrating unusual microsphere packing arrangements of 1 μm fluorescein-labeled core–shell–corona silica microspheres (batch B, see text) in approximately 3 μm by 4 μm rectangular-shaped pyramidal microwells caused by the kinetics of nucleation and crystallization of microspheres. Each of two series (a) to (c) and (d) to (f) are optical cross-sections descending from the top to the bottom of the microwells.

In this work with microwells, we routinely used high lateral resolution with frame size *ca.* 5 μm × 5–10 μm, unlike that commonly used in confocal microscopy, which uses scanning areas in the range of 50 × 50 μm.[10] As a result, photobleaching of FITC in our studies was exacerbated, affecting to a certain extent the image quality upon scanning a particular region more than once. This was only an issue for detailed imaging of unique microsphere packing arrangements such as shown in Fig. 4d–f.

Conclusion

In this study we have been able for the first time to obtain a complete map of the 3D lattice structure of microphotonic crystals in planarized opal-patterned silicon chips. The importance of the geometric constraints of square and rectangular shaped pyramidal microwell relief patterns in the surface of the silicon substrate as well as the microsphere filling conditions on the crystallization and packing of the microspheres in the microwells has been illustrated. This study has demonstrated that the laser scanning confocal microscopy technique offers a powerful capability of probing intimate details of the internal photonic lattice structure, degree of order and presence of defects in planarized opal-patterned chips in a non-destructive *in situ* mode of operation and with sub-micron spatial resolution. All of this speaks well for the use of laser scanning confocal microscopy as an *in situ* monitoring technique for elucidating planarized opal-patterned chip quality and chip yield. This methodology is envisioned to play an indispensable role in the future development of microphotonic crystal chips for possible use in highly compact optical telecommunication systems and maybe all-optical computers. A comprehensive study of microsphere packing in surface relief patterns of different substrates is currently underway.

Experimental

To obtain micron-size fluorescent labeled core–shell–corona silica microspheres an approach introduced by van Blaaderen and Vrij,[14] was combined with a controlled silica regrowth process.[4,15] A typical experimental procedure given for batch B was the following: 0.13 mL (0.55 mmol) of 3-aminopropyltrimethoxysilane (APS) was added to 25 mg of fluorescein isothiocyanate (FITC) (0.064 mmol) under magnetic stirring in a vial purged with dry nitrogen. 2 mL of ethanol was added to completely dissolve the reactants and the reaction was left overnight. Core silica particles of *ca.* 480 nm were obtained by reacting 6.25 mL (0.03 mol) of tetraethoxysilane (TEOS) with 7.2 mL of water and 10.8 mL of 28 wt.% ammonia solution in 76 mL of ethanol. To these core silica particles, 18 mL (0.086 mol) of TEOS and the reaction product of APS with FITC in ethanol were added dropwise simultaneously during 30 h. 36 mL (0.173 mol) of TEOS were then added during 60 h. Ammonia and water concentrations were kept constant

during TEOS addition. Particles were purified by a standard procedure of centrifugation and redispersion using first ethanol and then water. Judging by the pale-green color of the supernatant free of silica particles, the yield of FITC incorporation was high. Fluorescent core–shell–corona particles of batch B obtained in such a way present a diameter of *ca.* 1 μm (1020 ± 15 nm) measured by SEM with FITC distributed uniformly in depth from *ca.* 480 to 750 nm from the center of the silica particles. Batch A obtained similarly has a microsphere diameter of *ca.* 900 nm (910 ± 15 nm) with the dye distributed from *ca.* 420 nm to 680 nm from the center. For both batches, microsphere polydispersity estimated by SEM was lower than 2%.

Rectangular-shaped and square-shaped pyramidal microwells patterned within the surface of a 100 silicon wafer were prepared and filled with silica microspheres as described previously.[8] To achieve larger numbers of microsphere defects in microwells, non-optimal spin-coating parameters were used for this study, namely lower microsphere concentrations and higher spin-coating speeds.

A Zeiss LSM 510 confocal laser scanning microscope was used to obtain images of microspheres in microwells in 100 silicon wafers. FITC fluorescence was excited at 488 nm using a 200 mW Ar laser incorporated into the LSM 5 Zeiss laser module and emission light was collected from 505 to 550 nm centered around the FITC emission at *ca.* 525 nm. Maximum lateral resolution was achieved using a Zeiss 100× oil immersion objective with a numerical aperture of 1.4. The typical pinhole size was varied from 0.4 to 1.2 Airy units, therefore the thickness of the optical sections imaged was less than or comparable to the diameter of the microspheres. To minimize light scattering, the microwells were filled with ethylene glycol. Images were collected for a few seconds (typically 2 s) and frame-averaging techniques were used to increase the signal-to-noise ratio.

Acknowledgement

GAO is Government of Canada Research Chair in Materials Chemistry. He is deeply grateful to the Natural Sciences and Engineering Research Council NSERC, the Connaught Foundation and the University of Toronto for financial support of this research. Invaluable discussions with Dr. Hernán Míguez are deeply appreciated.

References

1 J. D. Joannopoulos, R. D. Meade and J. N. Winn, *Photonic crystals: molding the flow of light*, Princeton University Press, Princeton, NJ, 1995, p. 184.
2 Y. Xu, H. B. Sun, J. Y. Ye, S. Matsuo and H. Misawa, *J. Am. Opt. Soc. B - Opt. Phys.*, 2001, **18**, 1084.
3 A. Blanco, E. Chomski, S. Grabtchak, M. Ibisate, S. John, S. L. Leonard, C. López, F. Meseguer, J. P. Mondia, G. A. Ozin and O. ToaderH. M. Van Driel, *Nature*, 2000, **405**, 437.
4 H. Míguez, E. Chomski, F. García-Santamaría, M. Ibisate, S. John, C. López, F. Meseguer, J. P. Mondia, G. A. Ozin, O. Toader and H. M. van Driel, *Adv. Mater.*, 2001, **13**, 1634.
5 E. Chomski and G. A. Ozin, *Adv. Mater.*, 2001, **12**, 1071.
6 S. M. Yang and G. A. Ozin, *Chem. Commun.*, 2000, 2507.
7 M. Freemantle, *Chem. Eng. News*, 2001, **79**, 55.
8 S. M. Yang and G. A. Ozin, *Adv. Funct. Mater.*, 2001, **11**, 1.
9 A. Van Blaaderen, A. Imhof, W. Hage and A. Vrij, *Langmuir*, 1992, **8**, 1514.
10 U. Gasser, E. R. Weeks, A. Schofield, P. N. Pusey and D. A. Weitz, *Science*, 2001, **292**, 258.
11 K.-H. Lin, J. C. Crocker, V. Prasad, A. Schofield, D. A. Weitz, T. C. Lubensky and A. G. Yodh, *Phys. Rev. Lett.*, 1992, **8**, 2921.
12 A. Van Blaaderen, R. Ruel and P. Wiltzius, *Nature*, 1997, **385**, 321.
13 A. Van Blaaderen, *MRS Bull.*, 1998, **23**, 39.
14 A. Van Blaaderen and A. Vrij, *Langmuir*, 1992, **8**, 2921.
15 H. Giesche, *J. Eur. Ceram. Soc.*, 1994, **14**, 205.
16 A. D. Dinsmore, E. R. Weeks, V. Prasad, A. C. Levitt and D. A. Weitz, *Appl. Opt.*, 2001, **40**, 4152.
17 N. Hunt, R. Jardine and P. Bartlett, *Phys. Rev. E*, 2000, **62**, 900.